Large Scale Grid Integration of Photovoltaic and Energy Storage Systems Using Triple Port Dual Active Bridge Converter Modules

Viju Nair R*, Srinivas Gulur*, Ritwik Chattopadhyay*, Richard Beddingfield*, Shashank Mathur*,
Subhashish Bhattacharya*, Ghanshyamsinh Gohil†, Paul R. Ohodnicki‡
*FREEDM Systems Center, North Carolina State University, Raleigh, USA, †University of Texas, Dallas, USA
†National Energy Technology Laboratory, Pittsburgh, PA, USA.

***Abstract*—Integration of solar energy (PV) using isolated high frequency power electronic converters to the utility grid or micro-grid is fast becoming an attractive option due to the improvement in power density and elimination of the bulky low frequency transformer. This paper presents and analyzes the integration of solar energy and battery based energy storage system (ESS) to the grid using a two stage topology which includes triple port dual active bridges (DABs) and a conventional 2-level inverter. This paper considers the triple port DABs as the basic building blocks which can be connected in different configurations to meet the voltage and power requirements. Detailed simulation results are provided, investigating various operating and control modes. Experimental result showing the triple port DC-DC converter waveforms are also included. This paper shows that the triple port DAB modules along with the inverter is a viable option for large scale PV-ESS grid integration.**

***Index Terms*—DC-DC converter, dual active bridge (DAB), multi-winding transformer, control, photovoltaic, energy storage system.**

I. Introduction

The last few years have seen a significant rise in the number of large solar farms, each farm comprising of several panels, due to the reduction in production and installation cost [1]. These solar farms cannot be directly connected to the utility grid or the micro-grid due to the alternating nature of the grid voltage and have to be interfaced through a power electronic based converter. The integration to the utility grid or the micro-grid can be achieved by using a variety of power electronic converters in several different ways. Conventionally, the solar energy has been integrated to the grid using a two stage process which included a non-isolated DC-DC stage followed by an DC-AC stage [2], [3]. The galvanic isolation in such systems was typically provided by a low frequency transformer.

In the recent past, DABs have a become a popular option for being used as DC-DC converters due to their inherent soft-switching capability as well as their ability to provide galvanic isolation using a high frequency transformer [4]–[6]. The DC-AC stage can be realized by voltage source converters (VSCs), which have been very popular due the wide variety of functionality offered by them [7]. Some of the popular VSCs can be classified as 2-level, neutral point clamped (NPC), cascaded H Bridge (CHB), multi-modular converters (MMCs) etc [8]–[10].

This paper presents a grid integrated two stage topology consisting of two parallel connected triple port DABs integrated to a 2-level inverter. Each triple port DAB integrates a PV and a battery based energy storage through a multi-winding transformer. A energy storage has been included in this system to regulate the active power flow in-case of fluctuations in the solar energy. For this paper the battery based energy storage is isolated from the solar panels and hence a triple port DAB based topology has been be adopted [11]. Active power flow under different modes of operations have been analyzed.

The paper is organized as follows. Section II describes the topology as well as the operational aspects of the two stage grid interfaced system. Detailed simulation and preliminary experimental results have been presented in Section III and the conclusion and future work has been provided Section IV.

II. PV-ESS grid integration using triple port DAB DC-DC converter module as Building blocks

The DAB DC-DC converter topology is proven for high power density, bidirectional power flow, low device stresses, small filter components, low switching losses and improved efficiency [12]. The detailed analysis on the ZVS (zero voltage switching) range, the effect of magnetizing inductance and snubber capacitance in the ZVS range is discussed in [13]. In [14], the issue of circulating currents and hard switching at light loads is addressed with PWM control of the DAB. This

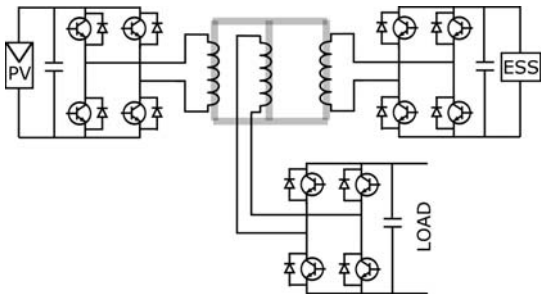

Fig. 1: A triple port DAB with PV, ESS and the output integrated using a HF transformer.

work extends the two port DAB to a three port DAB using PV-

978-1-5386-7703-2/18/$31.00 ©2018 IEEE

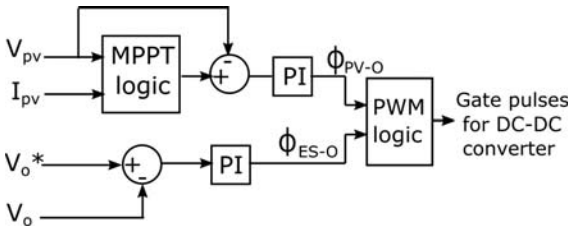

Fig. 2: Control strategy to determine the phase angles between the ports of the module

ESS as the two of the ports and the output port for connecting other loads as shown in Fig. 1. This integrated approach utilizes a single power conversion stage to interconnect the different ports which reduces the cost, size, volume and weight of the whole system, resulting in improved power density and efficiency. To obtain fast dynamic response, decoupled power flow analysis for a triple port DAB is done in [15]. The ZVS characteristics of independent power flow control of triple port DAB converter is detailed in [16], [17]. Another important consideration is the design of the HF transformer used in the triple port DAB. The modeling, design and analysis of three limb HF transformer is provided in [18]. Also the split winding type transformer approach with wide ZVS range and to mitigate the limitation of power flow when one of the three port is idle, is discussed in [19]. The phase shift control is used for controlling the power flow between the ports of three port DAB DC-DC converter and the control scheme shown in Fig. 2 is used to determine the relative phase angles between the two ports. The MPPT algorithm optimizes the energy yield of the PV array. Perturb and observe algorithm has been implemented and it gives the reference PV array voltage to extract maximum power from the PV array. The PI controller is designed to track the PV array voltage to the reference voltage by adjusting the phase angle between the AC output voltages of the PV H-bridge and the output H-bridge of the three port DC-DC converter. Since the power drawn by the load (grid connected inverter) is independent, the environmental conditions (solar radiance, temperature) and MPPT logic may lead to variation in the output voltage. Therefore the output voltage is controlled by balancing the PV power and load demand using the energy storage systems (battery bank in this work). This DC-DC module can be

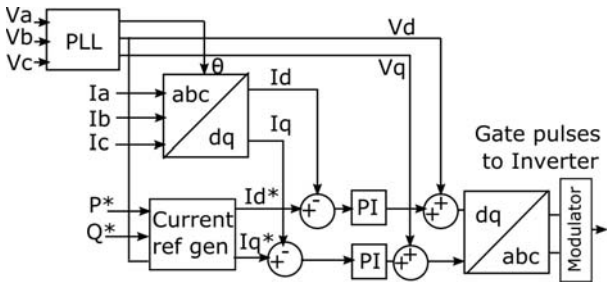

Fig. 3: Simplified control scheme for the current control of the grid connected inverter.

interfaced to an inverter and connected to grid. Since the DC-DC module is capable of maintaining the DC link voltage, the inverter has more degrees of freedom and provides better resiliency and redundancy compared to systems with PV alone. The grid connected inverter is controlled by transforming the feedback and control variables in the rotating reference frame. Phase locked loop (PLL) is used for the grid voltage space vector angle detection and synchronization. Since the output voltage is regulated using the DC-DC converter, the grid connected inverter is controlled to inject/draw desired amount of active and reactive power to the grid. From the reference active and reactive power command, q-axis and d-axis components of the reference current are calculated. The PI controllers are used to track the reference current as shown in Fig 3. Depending on the availability of PV power, ESS energy status and load demand, six different control modes are possible as shown in Fig. 5. Also, it should be noted that the PV operate in non MPPT mode if the load demand is not high and if the ESS is already charged. There is a seamless transfer between these different operating modes which is shown in the simulation results in the next section. In this figure, the output of the triple port DC-DC module is directly connected to the inverter but for large scale power flow, multiple modules can be connected in series, parallel (Fig. 4) or in series-parallel arrangement, depending on the voltage level also.

The striking feature of this PV-ESS grid integration using triple port DAB converters is in its modularity. Even if any module fails, the system can still operate with reduced power and with different output voltages per module. Similarly, the power levels can be scaled up by adding additional modules. As previously mentioned, the DC link voltage is maintained by the DC-DC module itself and the inverter is capable of meeting any new grid connection requirements suggested by IEEE 1547. These modules with the rated power level are standard power electronic converters which can be replicated and this reduces the cost. Absence of low frequency transformer is another advantage.

III. Simulation and Experimental results

The schematic shown in Fig. 4 is simulated with parameters mentioned in Table-I and the results are presented in this

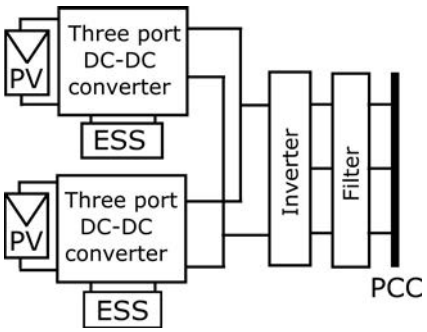

Fig. 4: Grid integration using parallel connected triple port DAB modules.

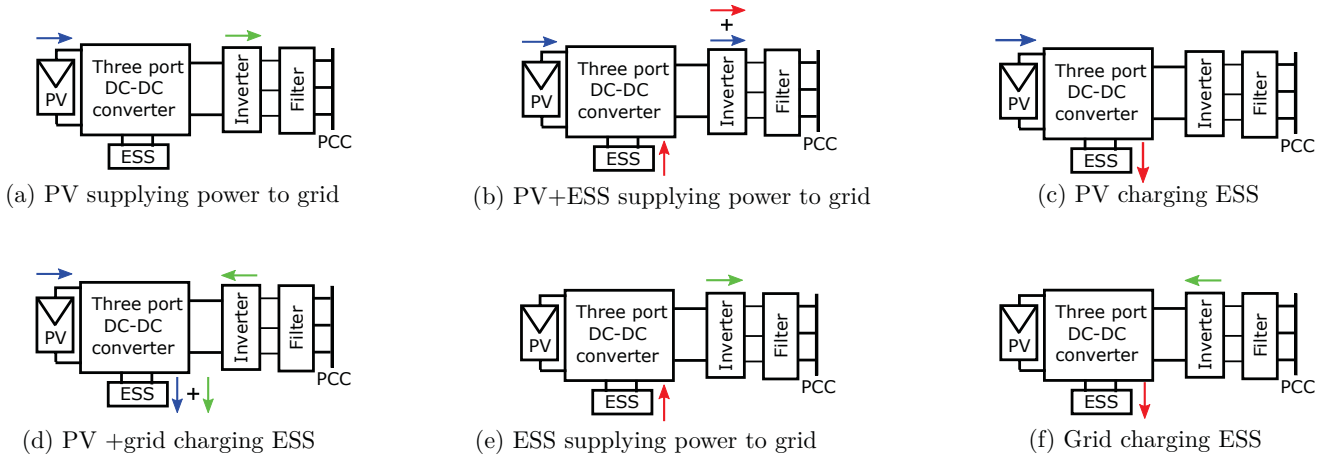

(a) PV supplying power to grid (b) PV+ESS supplying power to grid (c) PV charging ESS

(d) PV +grid charging ESS (e) ESS supplying power to grid (f) Grid charging ESS

Fig. 5: Different possible control modes - interaction of PV, ESS and the grid.

section. The simulation mainly focuses on the basic operation of the triple port DAB module, the response of the system with varying load demand and also on the occurrence of any fault in the ac side.

TABLE I: Simulation Parameters

Parameter	Value
Power Rating	100 kW
Grid voltage	480 V
Grid frequency	60 Hz
Converter side inductance	600 uH
AC side filter capacitance	46 uF
Grid side filter inductance	90 uH
Inverter switching frequency	5 kHz
DC-DC converter module power	50 kW
DC-DC converter switching frequency	10 kHz
Transformer leakage	60 uH
PV port power, voltage	50 kW, $600 - 1000$ V
Battery power, voltage	50 kW, $480 - 672$ V
Output voltage	800 V

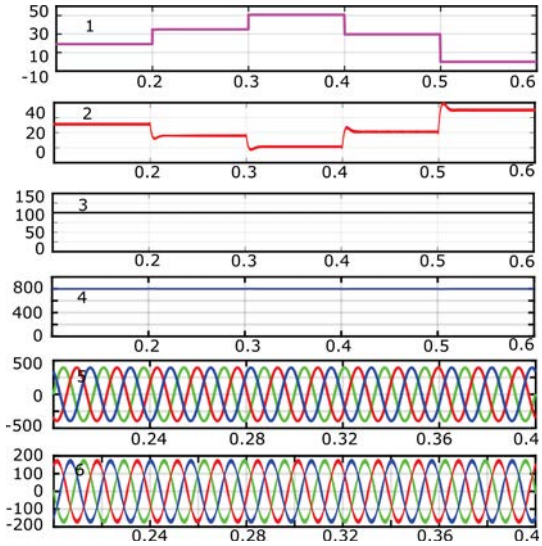

Fig. 6: Operation of the triple port DAB for meeting the base load under varying irradiance. 1. MPPT power (kW) per module, 2. Battery power (kW) per module, 3. Total power injected to grid (kW), 4. DC link voltage (V), 5. Grid voltage (V), 6. Grid current (A). x-axis is time in seconds.

Fig. 6 shows the base load operation where in the grid demands constant 100KW and the PV power is varied as shown in trace-1. It can be seen that the battery power (trace-2) changes in such a way that always the grid demand is met and in this process the DC link voltage (trace-4) is maintained as well. For instance, from 0.3 to 0.4s, when each of the PV module is supplying the 50kW, the battery power goes to 0 since the grid demand is met using the PV modules alone.

Fig. 7 shows the case when the load demanded is varying along with varying PV power. This results shows the more general cases, which includes both the battery charging and discharging. Initially, both the PV (trace-4) and the battery (trace-5) is supplying 25kW each per module to meet the 100kW grid demand (trace-1). At 0.3s, there is no load demand. Therefore the PV power is used to charge the battery and its power goes to -25kW per module. At 0.4s, both the PV and the grid charges the battery and at 0.5s, when there is no PV power, grid alone charges the battery. These simulation results also shows the proper working and stability of the control system used for the triple port DAB modules in PV-ESS grid integration.

Fig. 8 shows how PV-ESS module responds on the occurrence of a three phase fault at the PCC to comply with the grid connection standards. The total load demanded is 50kW prior to the fault. At 0.1s, a three phase fault occurs at the PCC and the PCC voltage drops to half of the rated value. During this fault occurrence, the inverter is commanded to stop injecting any active power (id) to grid and also supply the reactive power (iq) to support the grid. Since the active power injection is zero, the available PV power (trace-4) which is 25kW is used to charge the battery (trace-5) during this time which goes to -25kW. Above simulation result also shows the current controlled operation of the inverter.

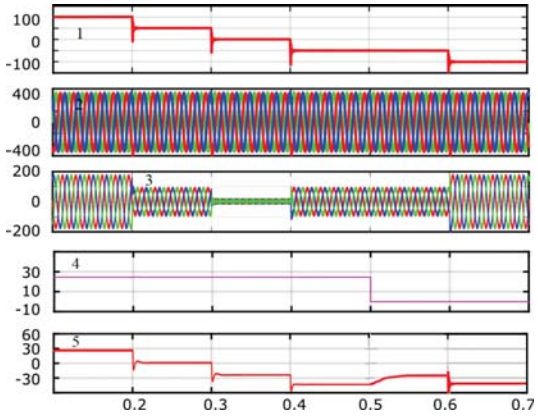

Fig. 7: Operation of the triple port DAB for meeting the varying load demand under varying PV power. 1. Total injected grid power (kW), 2. Grid voltage (V), 3. Grid current (A), 4. MPPT power (kW) per module, 5. Battery power (kW) per module. x-axis is time in seconds.

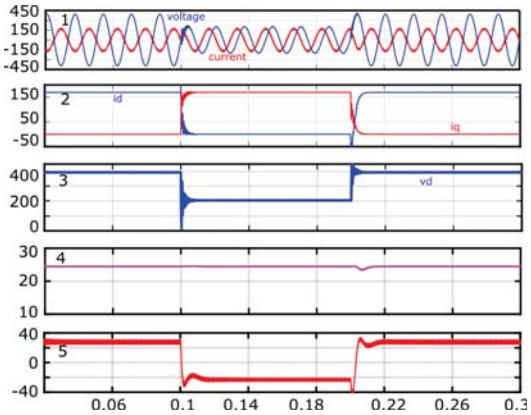

Fig. 8: Operation of the triple port DAB on the occurrence of a three phase fault. 1. Grid voltage (v) and grid current (A), 2. d-axis (id) and q-axis currents (iq), 3. d-axis voltage (vd), 4. PV power (kW) per module. 5. Battery power (kW) per module. x-axis is time in seconds.

Laboratory prototype is developed for the DC-DC triple port DAB and tested for 10kW. The 10kW, 100KHz transformer based on 3C97 ferrite core is shown in Fig. 9. The design details of the HF transformer including the leakage inductances, turns, size and power density are also provided in the figure. The experimental result showing the voltages across the windings and the winding currents are provided in the Fig. 10. The phase shift between the winding voltages shows the direction of power flow.

The grid connected 2-level inverter current control is tested by building a laboratory based hardware prototype as shown in Fig.11. Fig.12 shows the 3ϕ, ac grid voltages and currents of the grid interconnected voltage source based inverter.

IV. Conclusion

This paper presents a PV-ESS integrated DC-DC triple port converter modules as building blocks for large scale PV-ESS integration to grid. The ZVS operation, high power density, galvanic isolation, seamless transfer between the different operating modes and the modular nature are the notable features of the triple port DAB based DC-DC converter modules. Since the DC-DC converter maintains the DC link voltage, the inverter has additional degrees of freedom to meet the existing and the newer regulations in IEEE 1547 standards. Also, the power level can be scaled up by adding additional modules with much ease. All these features make this PV-ESS integrated triple port DAB converter interfaced to an inverter a very attractive solution for large scale PV integration to grid.

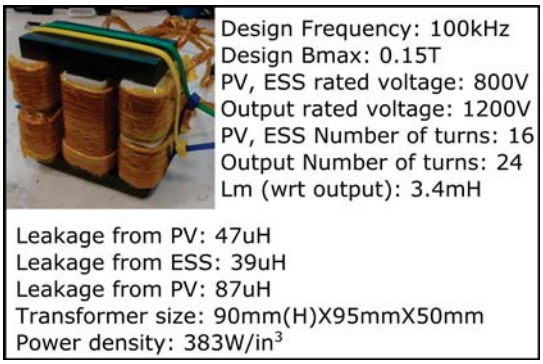

Fig. 9: Laboratory prototype of the 10kW, 100kHz transformer and its design parameters.

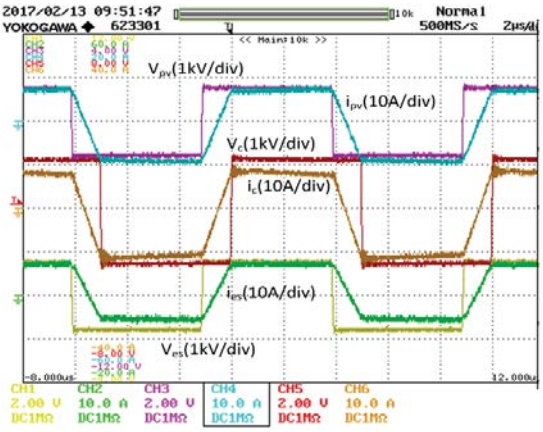

Fig. 10: Experimental result showing the winding voltages and the currents. Vpv, ipv, Ves, ies, Vc, ic refers to the voltages and currents of PV, ESS and the output side.

V. Acknowledgement

This work made use of FREEDM ERC shared facilities supported by NSF.

References

[1] T. Stetz, F. Marten, and M. Braun, "Improved low voltage grid-integration of photovoltaic systems in germany," *IEEE Transactions on Sustainable Energy*, vol. 4, no. 2, pp. 534–542, April 2013.

[2] A. Yazdani, A. R. D. Fazio, H. Ghoddami, M. Russo, M. Kazerani, J. Jatskevich, K. Strunz, S. Leva, and J. A. Martinez, "Modeling guidelines and a benchmark for power system simulation studies of three-phase single-stage photovoltaic systems," *IEEE Transactions on Power Delivery*, vol. 26, no. 2, pp. 1247–1264, April 2011.

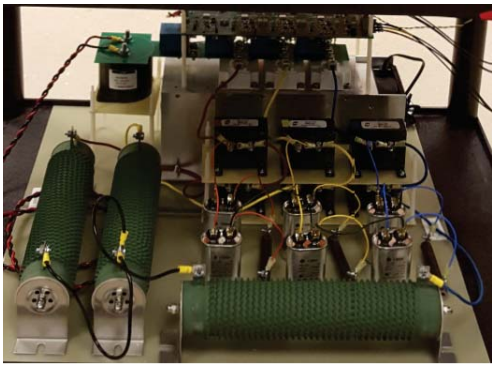

Fig. 11: Laboratory based hardware prototype for the 2-level, 3ϕ voltage source inverter.

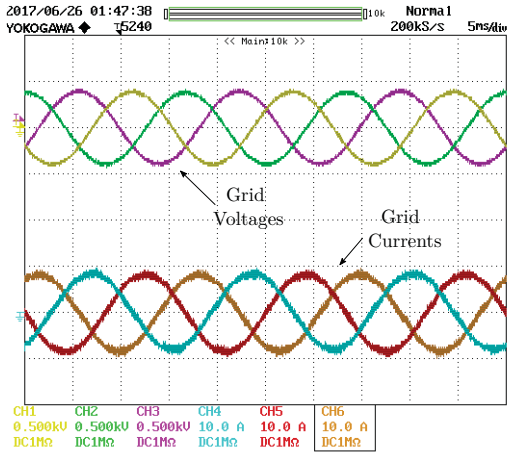

Fig. 12: Grid voltage and current waveforms for the 2-level, 3ϕ voltage source inverter.

[3] E. Figueres, G. Garcera, J. Sandia, F. Gonzalez-Espin, and J. C. Rubio, "Sensitivity study of the dynamics of three-phase photovoltaic inverters with an lcl grid filter," *IEEE Transactions on Industrial Electronics*, vol. 56, no. 3, pp. 706–717, March 2009.

[4] M. N. Kheraluwala, R. W. Gascoigne, D. M. Divan, and E. D. Baumann, "Performance characterization of a high-power dual active bridge dc-to-dc converter," *IEEE Transactions on Industry Applications*, vol. 28, no. 6, pp. 1294–1301, Nov 1992.

[5] G. G. Oggier, G. O. Garca, and A. R. Oliva, "Switching control strategy to minimize dual active bridge converter losses," *IEEE Transactions on Power Electronics*, vol. 24, no. 7, pp. 1826–1838, July 2009.

[6] F. Krismer and J. W. Kolar, "Efficiency-optimized high-current dual active bridge converter for automotive applications," *IEEE Transactions on Industrial Electronics*, vol. 59, no. 7, pp. 2745–2760, July 2012.

[7] J. Rodriguez, J.-S. Lai, and F. Z. Peng, "Multilevel inverters: a survey of topologies, controls, and applications," *IEEE Transactions on Industrial Electronics*, vol. 49, no. 4, pp. 724–738, Aug 2002.

[8] J. Rodriguez, S. Bernet, B. Wu, J. O. Pontt, and S. Kouro, "Multilevel voltage-source-converter topologies for industrial medium-voltage drives," *IEEE Transactions on Industrial Electronics*, vol. 54, no. 6, pp. 2930–2945, Dec 2007.

[9] R. Marquardt, "Modular multilevel converter: An universal concept for hvdc-networks and extended dc-bus-applications," in *The 2010 International Power Electronics Conference - ECCE ASIA -*, June 2010, pp. 502–507.

[10] J. Rodriguez, S. Bernet, P. K. Steimer, and I. E. Lizama, "A survey on neutral-point-clamped inverters," *IEEE Transactions on Industrial Electronics*, vol. 57, no. 7, pp. 2219–2230, July 2010.

[11] C. Zhao, S. D. Round, and J. W. Kolar, "An isolated three-port bidirectional dc-dc converter with decoupled power flow management," *IEEE Transactions on Power Electronics*, vol. 23, no. 5, pp. 2443–2453, Sept 2008.

[12] R. W. A. A. D. Doncker, D. M. Divan, and M. H. Kheraluwala, "A three-phase soft-switched high-power-density dc/dc converter for high-power applications," *IEEE Transactions on Industry Applications*, vol. 27, no. 1, pp. 63–73, Jan 1991.

[13] M. H. Kheraluwala, R. W. Gasgoigne, D. M. Divan, and E. Bauman, "Performance characterization of a high power dual active bridge dc/dc converter," in *Conference Record of the 1990 IEEE Industry Applications Society Annual Meeting*, Oct 1990, pp. 1267–1273 vol.2.

[14] A. K. Jain and R. Ayyanar, "Pwm control of dual active bridge: Comprehensive analysis and experimental verification," *IEEE Transactions on Power Electronics*, vol. 26, no. 4, pp. 1215–1227, April 2011.

[15] C. Zhao, S. D. Round, and J. W. Kolar, "An isolated three-port bidirectional dc-dc converter with decoupled power flow management," *IEEE Transactions on Power Electronics*, vol. 23, no. 5, pp. 2443–2453, Sept 2008.

[16] R. Chattopadhyay and S. Bhattacharya, "Power flow control and zvs analysis of three limb high frequency transformer based three-port dab," in *2016 IEEE Applied Power Electronics Conference and Exposition (APEC)*, March 2016, pp. 778–785.

[17] Ritwik and S. Bhattacharya, "Zvs analysis and power flow control for three limb transformer enabled sic mosfet based three port dab integrating pv and energy storage(es)," in *2016 IEEE Energy Conversion Congress and Exposition (ECCE)*, Sept 2016, pp. 1–8.

[18] R. Chattopadhyay, M. A. Juds, P. R. Ohodnicki, and S. Bhattacharya, "Modelling, design and analysis of three limb high frequency transformer including transformer parasitics, for sic mosfet based three port dab," in *IECON 2016 - 42nd Annual Conference of the IEEE Industrial Electronics Society*, Oct 2016, pp. 4181–4186.

[19] R. Chattopadhyay, G. Gohil, and S. Bhattacharya, "Split-winding type three limb core structured hf transformer for integrating pv and energy storage(es)," in *2017 IEEE Applied Power Electronics Conference and Exposition (APEC)*, March 2017, pp. 2997–3004.